Available online at www.sciencedirect.com
SCIENCE DIRECT®
ELSEVIER
Journal of Magnetism and Magnetic Materials 301 (2006) 521–526
Journal of magnetism and magnetic materials
www.elsevier.com/locate/jmmm

Electrical transport and magnetic properties of perovskite-type electron-doped La–Pr–Mn–O epitaxial films

Ping Duan[a,b,*], Zhenghao Chen[b,1], Shouyu Dai[b,c], Lifeng Liu[b], J. Gao[c]

[a]*Department of Physics, Tianjin University, Tianjin 300072, China*
[b]*Laboratory of Optical Physics, Institute of Physics and Center for Condensed Matter Physics, Chinese Academy of Sciences, P.O. Box 603, Beijing 100080, China*
[c]*Department of Physics, The University of Hong Kong, Pokfulam Road, Hong Kong, China*

Received 5 May 2005; received in revised form 26 July 2005
Available online 25 August 2005

Abstract

$La_{1-x}Pr_xMnO_3$ (LPrMO) thin films have been epitaxially grown on (1 0 0)$SrTiO_3$ single-crystal substrates by pulsed-laser deposition. The films have a perovskite structure and give rise to the colossal magnetoresistance effect with the maximum magnetoresistance ratio of 10^3% (at 240 K and 5 T). The electrical transport and magnetic properties have been investigated for the $La_{0.8}Pr_{0.2}MnO_3$ film with thickness 3000 Å. The results indicate that the films have quite a distinctive magnetotransport behavior compared to the bulk. The analysis of X-ray photoemission spectroscopy suggests that the valence state of Pr is 4+ in LPrMO film. Therefore, the epitaxial film is most likely an electron-doped colossal magnetoresistance system.

PACS: 75.47.GK; 75.70.AK; 72.80.Ga

Keywords: Thin films; Transport properties; Magnetic properties

1. Introduction

Rare-earth-doped manganites $La_{1-x}A_xMnO_3$ and their corresponding films fabricated using different methods with a colossal magnetoresistance (CMR) effect have been widely investigated due to their remarkable magnetic and transport properties as well as their applications to magnetic memory sensor, read heads, etc. However, they are

*Corresponding author. Department of Physics, Tianjin University, Tianjin 300072, China. Tel.: +86 2227405053; fax: +86 1082649531.
E-mail addresses: ppingduan@yahoo.com.cn (P. Duan), zhchen@aphy.iphy.ac.cn (Z. Chen).
[1]Also to be corresponded to.

0304-8853/$ - see front matter © 2005 Elsevier B.V. All rights reserved.
doi:10.1016/j.jmmm.2005.08.003

usually hole-doped compounds in which La^{3+} ions of the parent compound $LaMnO_3$ are substituted by divalent A^{2+} (Ca^{2+}, Sr^{2+}, Ba^{2+}, etc.) or univalent ions A^{1+} (Na^{1+}) [1], and Mn has a mixed state of Mn^{3+} ($t_{2g}^3e_g^1$) and Mn^{4+} ($t_{2g}^3e_g^0$). If a tetravalent A^{4+} or pentavalent A^{5+} cation is substituted in the La site, then Mn^{3+} ($t_{2g}^3e_g^1$)–O–Mn^{2+} ($t_{2g}^3e_g^2$) system is obtained and the carriers are electrons. Recently these electron-doped manganites have attracted much interest, and Ce^{4+}, Te^{4+}, Sb^{5+} doped in $LaMnO_3$ have been reported [2–8]. It can be predicted this kind of n-type CMR manganite will come to have much significance for both fundamental and applied research. A combination of electron- and hole-doped ferromagnetic manganites may open up possibilities for fabricating bipolar devices [2] and is promising for novel functional spintronics devices in future.

In our previous work [9], a new polycrystalline compound $La_{1-x}Pr_xMnO_3$ (LPrMO) synthesized using solid-state reaction in which rare-earth element La was substituted by rare-earth element Pr could be viewed as electron-doped single-perovskite-phase manganite. It is well known that Pr_6O_{11}, with Pr state of Pr^{3+} (1/3 mol percent) and Pr^{4+} (2/3 mol percent) mixing valent state, is most stable at room temperature for all oxides of praseodymium. Therefore, it is probable that the valence states of Pr are composed of Pr^{3+} and Pr^{4+} in manganites, which enable an investigation on electrical transport and magnetic properties of single-textured LPrMO. In this letter, we investigated LPrMO thin films deposited by pulsed laser deposition (PLD) method. The results indicated that single-textured epitaxial thin films were fabricated successfully under optimal growth conditions in our experiments. As a result, we found that the films had quite a distinctive magnetotransport behavior from the bulks, and the CMR effect was enhanced drastically in the films.

2. Experiment and structure

Sintered targets LPrMO for PLD were prepared using the conventional ceramic technique. LPrMO bulks were prepared following the standard ceramic process. Stoichiometric mixtures of high-purity La_2O_3, Pr_6O_{11} and $MnCO_3$ powders were presintered at 1073 K for 12 h, calcined at 1203 K for 24 h, 1373 K for 24 h, and 1473 K for 12 h. Finally, the resulting bars were sintered at 1573 K for 12 h and furnace cooled to room temperature. Epitaxial LPrMO films were fabricated using a PLD equipment. In the PLD processing, a XeCl excimer laser beam (308 nm, 20 ns, 6 Hz, 2 J/cm^2) was used as the deposition light source. The targets were mounted on a rotating holder, 40 mm away from the $SrTiO_3$ substrates. Several substrate temperatures and deposition pressures were used in order to obtain single-phase and metal–insulator transition (MIT) in the films. The optimal conditions for growing the films in our experiment was that, the deposition chamber was vacuumed to a base pressure of 5×10^{-4} Pa at the beginning, and then during growth, a pure pressure of oxygen was kept at 0.3 Torr. The substrate temperature was maintained at 750 °C, and the films were slowly cooled down to room temperature after deposition.

In this letter, $La_{0.8}Pr_{0.2}MnO_3$ thin films with a thickness of 3000 Å grown on single-crystal (1 0 0)$SrTiO_3$ substrates were investigated. The crystal structure of the films was analyzed by means of X-ray diffraction (XRD). Energy dispersion spectroscopy (EDS) and inductively coupled plasma–atomic emission spectroscopy (ICP–AES), with error limits less than 2%, were used to determine the composition of the films. The electrical resistivity of the films was measured by the conventional 4-probe technique from 5 to 310 K in a field up to 5 T. Magnetic measurements were carried out with a super-conducting quantum interference device (SQUID) magnetometer. In all measurements, the applied field was parallel to the film plane. To study the electronic states of the films, X-ray photoemission spectroscopy (XPS) was also performed.

The typical XRD pattern of the LPrMO films is shown in Fig. 1. The presence of only (0 0 *l*) peaks in the XRD patterns indicates that the films have a perovskite single-phase structure with a uniaxial orientation. The full-width at half-maximum (FWHM) of the (0 0 2) peak for the films is about 0.3°. On the other hand, according to the result of

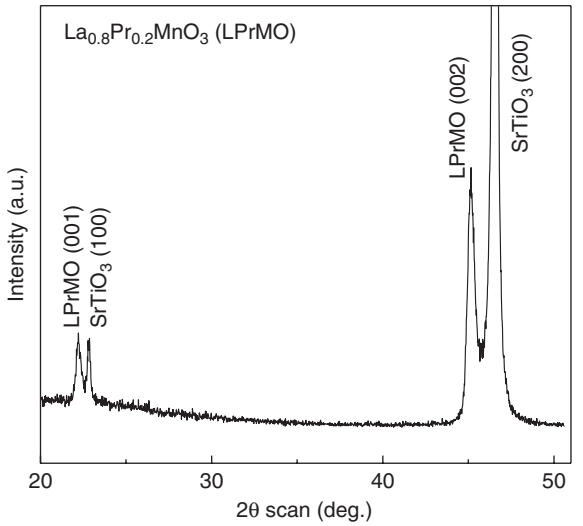

Fig. 1. XRD pattern of $La_{0.8}Pr_{0.2}MnO_3$ thin film epitaxially grown on (1 0 0) $SrTiO_3$.

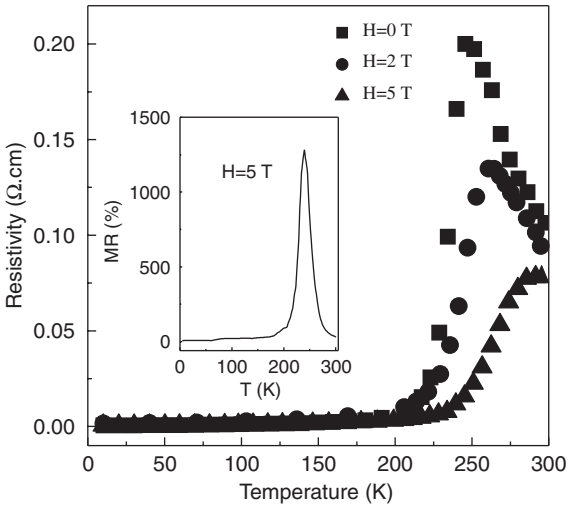

Fig. 2. Temperature dependence of the electrical resistivity for $La_{0.8}Pr_{0.2}MnO_3$ thin film under applied magnetic fields 0, 2, and 5 T, respectively; the MR ratio for the film is displayed in the corresponding inset.

the quantitative EDS and ICP–AES analyses, the composition of presented $La_{0.8}Pr_{0.2}MnO_3$ films is very close to the nominal composition, and can be viewed as $La_{0.8}Pr_{0.2}MnO_{3-\delta}$ in which the deviation of oxygen content δ is very small, about 0.01.

3. Results and discussion

3.1. Electrical transport properties

Fig. 2 presents the temperature dependence of the resistivity ($\rho(T)$) of $La_{0.8}Pr_{0.2}MnO_3$ thin film under the applied magnetic fields of 0, 2, and 5 T. As shown in Fig. 2, $\rho(T)$ exhibits a unique and very sharp MIT, and the transition temperature T_{MI} is about 250 K at zero field. At temperatures above T_{MI}, $\rho(T)$ decreases with increasing temperature, which indicates that the conduction occurs via a thermal activated process. It is noteworthy that $\rho(T)$ decreases rapidly under T_{MI} and the residual resistivity is very small at low temperatures, which is a characteristic of high-quality films [10,11]. When magnetic field is applied, $\rho(T)$ is suppressed significantly and T_{MI} becomes higher. Besides, the magnetoresistance (MR) is also small at low temperatures associated with the high degree of texture of the film that behaves similar to bulk single-crystal manganites. The MR ratio, calculated by $[(\rho_0 - \rho_H)/\rho_H]$, where ρ_H is the resistivity under an applied magnetic field, gets up to 1300% for the sample. The large value suggests that LPrMO thin film is a promising CMR material with potential applications [12].

In addition, it is evident that, as compared with the LPrMO bulk [9], the resistivity of the films decreases drastically, at the same time T_{MI} rises to 250 K at 0 T, and the CMR effect is enhanced significantly in the films. Furthermore, the upturn feature in $\rho(T)$ at low temperatures for the bulks (see Ref. [9], Fig. 2) also disappears for the films, confirming that the films are highly textured. These characteristics reflected the single crystalline or at least the highly textured nature of the films and are thought to be tied up with the fabrication method of PLD [13–15], which is a very none-quilibrium method of deposition that can lead to new properties compared to ceramics. Taking into account the analysis of XPS results (discussed later), we suggest that Pr ions in the LPrMO film system deposited using PLD under instantaneous high-energy operation is far from Pr^{3+} and almost in Pr^{4+} state, which bring about the transport improvement and enhancement of CMR effect.

The transport behavior of the films was analyzed by polynomial expansions at low temperatures. The $\rho(T)$ curves can be fitted by

$$\rho(T) = \rho_0 + \rho_E T^2 + \rho_M T^{4.5}, \quad (1)$$

where ρ_0 is the temperature-independent resistivity term, the T^2 and $T^{4.5}$ terms usually have been ascribed to electron–electron scattering [16] and electron–magnon scattering in manganites [17], respectively. Electron–electron scattering coefficient $\rho_E = 2.94 \times 10^{-6}\,\Omega\,\mathrm{cm/K^2}$ derived for our LPrMO thin film sample at zero field is comparable to $La_{1-x}Ca_xMnO_3$ (LCaMO) thin films [18] and the electron–magnon scattering coefficient $\rho_M = 5.5 \times 10^{-12}\,\Omega\,\mathrm{cm/K^2}$ is much smaller than ρ_E, suggesting the resistivity originates mainly from electron–electron scattering in the LPrMO film system. When an external magnetic field is applied, it is observed that the coefficients of ρ_0, ρ_E and ρ_M decrease with an increase in magnetic field. It indicates that the field drives the local momentum of Mn ions to orient in the direction of the applied magnetic field, hence reduces the electron and magnon scattering of carriers. On the other hand, at high temperatures except near T_{MI}, the $\rho(T)$ curves can be fitted well with the small polaron hopping model [19] and the activation energy is about 115 meV at zero field.

Fig. 3 presents the field dependence of ρ at different temperatures (normalized by the zero-field value). With increasing temperature, an increased negative MR is observed. Note that ρ varies almost linearly with the field, indicating there is no so-called large low-field MR (LFMR) behavior in the films. It is known that LFMR derived from spin-polarized electron tunneling mechanism between adjacent grains is often found in polycrystalline rather than single-crystalline samples [20]. LFMR is also found existing in LPrMO polycrystalline bulks [9] whereas not in the films of $La_{0.8}Pr_{0.2}MnO_3$. Therefore, this difference between the films of $La_{0.8}Pr_{0.2}MnO_3$ and bulks also implies the CMR effect in crystalline LPrMO films originates only from the intrinsic MR effect.

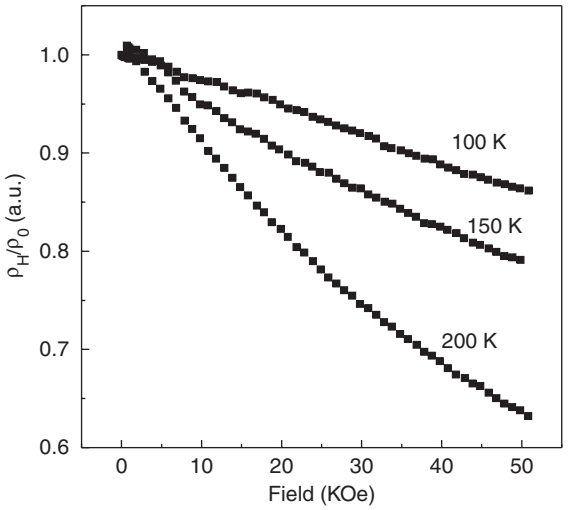

Fig. 3. Magnetic field dependence of the resistivity normalized to the 0 T value measured at temperatures of 100, 150, and 200 K, respectively.

3.2. Magnetic properties

The magnetization (M) vs. temperature (T) curves of the sample are shown in Figs. 4(a) and (b), taken at 10 kOe and 100 Oe, respectively. In Fig. 4(a), there is a transition from ferromagnetic (FM) to paramagnetic (PM) state in the M–T curve at Curie temperature T_c, which is obtained as the minimum of the curve dM/dT calculated from the measured field-cooled (FC) curves, a little lower than the temperature of MIT. The inset of Fig. 4(a) shows the magnetic field dependence of the magnetization at 5 K, which confirms the FM state of the thin films at low temperatures. After the sample was zero-field-cooled (ZFC) and FC down to 5 K, the thermomagnetization curve M–T was measured in a warming process at a field of 100 Oe as shown in Fig. 4(b), where the ZFC curve coincides with the FC curve at high temperature, but deviates from the FC trace and drops below a freezing temperature T_f (about 150 K). This irreversibility indicates that the magnetic moments are frozen at $T < T_f$ in ZFC process measurement, which is a telling feature of spin glass (SG) without simple long-range FM order in this system. This SG feature also appears in $La_{1-x}Te_xMnO_3$ epitaxial films [21]. Based on our results of LPrMO thin

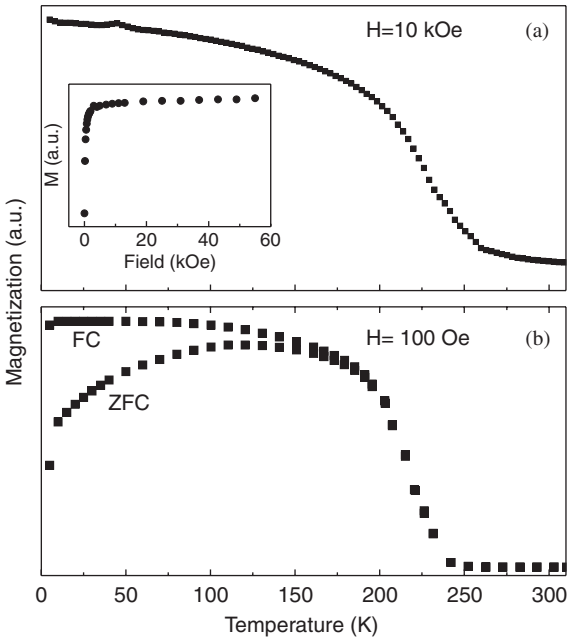

Fig. 4. Temperature dependence of magnetization at (a) 10 kOe in FC process and (b) 100 Oe in ZFC and FC processes. The inset of (a) shows the magnetic field dependence of the magnetization at 5 K.

films, this SG behavior of magnetism may come from the following respects. First, the effective radius of Pr^{4+} (0.10 nm) is smaller than that of La^{3+} (0.122 nm), causing intrinsic strain that reduces the Mn–O–Mn bond angle (from 180°). Second, the tensile strain arising from the lattice mismatch between the $La_{0.8}Pr_{0.2}MnO_3$ films and the $SrTiO_3$ substrate can also distort MnO_6 octahedron by elongating in-plane lattice parameters and shortening out-of-plane lattice parameter. The effect of the strain may probably weaken the double exchange interaction, thus favoring the antiferromagnetic superexchange interaction. Consequently, both double-exchange and superexchange interactions will compete more strongly, with dependence on the structural distortion, giving rise to a magnetically disordered state [22]. In LPrMO films, we suggest the intrinsic and extrinsic strains could play an important role in the SG properties. More study is essential in order to ascertain the microscopic natures and underlying physics of this SG-like behavior in LPrMO system.

3.3. XPS analysis

To explore the effect of the praseodymium doping in the LPrMO system, we obtained XPS pattern of the $La_{0.8}Pr_{0.2}MnO_3$ film using the Beijing Synchrotron Radiation Facility multitechnique spectrameter with a base gas pressure of 6.3×10^{-7} Pa at room temperature. Fig. 5(a) presents the spectrum of the O 1s core level. The O 1s peak at 528.4 eV is almost a single peak, which shows the cleanness of the surface, or the amount of contamination is small enough for us to analyze the spectra. In addition, the broad feature at about 537 eV probably arises from the La MNN Auger spectrum. Fig. 5(b) presents the valence band (VB) photoemission spectra taken at various photon energies of 65, 70, 80, 100, and 150 eV. The most prominent peaks are about 6.1 (peak A) and 3.7 eV (peak B) below E_F. Note that there is a low-intensity shoulder close to E_F marked by the arrows, which is similar to the VB spectra of $La_{1-x}Sr_xMnO_3$ [23], and the tail of the shoulder runs close to E_F suggesting the Fermi level of this material is close to the top of the VB. On the other hand, the VB spectral weight is shifted to low binding energy with the increasing photon energy,

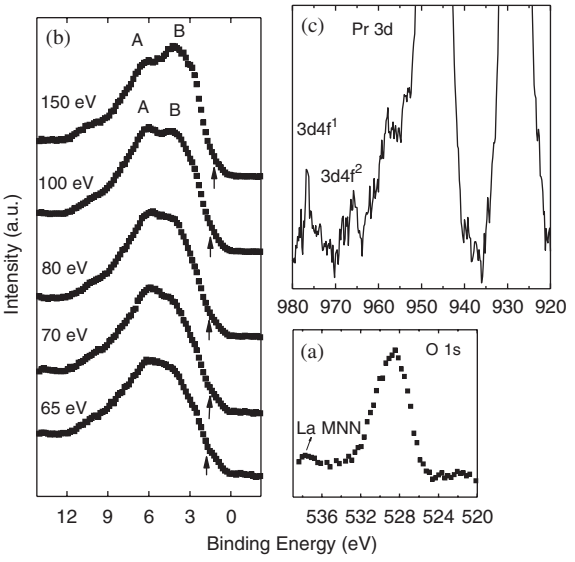

Fig. 5. (a) O 1s core level XPS spectrum. (b) Valence band XPS spectra taken at $h\upsilon = 65$, 70, 80, 100, and 150 eV. (c) Pr 3d core level XPS spectrum.

which is because the relative photoionization cross-section of O 2p compared with Mn 3d decreases as the photon energy increases [24]. Thus, it is deduced that the structure at 6.1 eV is dominated by the O 2p character and the structure at 3.7 eV results mainly from the Mn 3d states. Moreover, the VB of our films also revealed the extensive hybridization between Mn and O orbital. The XPS spectra of Pr 3d, is shown in Fig. 5 (c), in which one can clearly see the satellite peaks near 976 and 965 eV in the Pr $3d_{3/2}$ spectrum attributed to $3d4f^1$, $3d4f^2$ final states [25], respectively, which justifies the existence of Pr^{4+} ions in the samples because these satellite features are attributed to Pr^{4+}, and not observed in pure Pr^{3+} systems [25,26]. Therefore, Pr 3d XPS suggests the $La_{0.8}Pr_{0.2}MnO_3$ thin film with a single perovskite phase is most likely an electron-doped system. From XPS and the analysis of transport and magnetic properties, it may be concluded that Pr ions in LPMO thin films probably all exist in Pr^{4+} state, at least far from Pr^{3+}, which is not like in bulks where Pr^{3+} plays an important role in FM insulating state.

4. Conclusion

In summary, perovskite-type $La_{0.8}Pr_{0.2}MnO_3$ thin films were successfully fabricated by PLD technique. The MR characteristic of the $La_{0.8}Pr_{0.2}MnO_3$ epitaxial thin films shows a CMR behavior with a maximum ratio of 10^3%. Furthermore, we have found transport behavior reflects the single crystalline nature of the films by comparing with the results of the bulk one. The deviation of FC and ZFC magnetizations indicates the existence of spin glass-like behavior in $La_{0.8}Pr_{0.2}MnO_3$ films. With analysis of XPS, we suggest that the praseodymium in our system is in the 4+ valence state and therefore, $La_{0.8}Pr_{0.2}MnO_3$ thin films are most likely an electron-doped CMR material. The results show that the perovskite-type LPrMO film is a promising CMR material for theoretical research and technological applications.

References

[1] M. Itoh, T. Shimura, J.-D. Yu, T. Hayashi, Y. Inaguma, Phys. Rev. B 52 (1995) 12522.
[2] C. Mitra, P. Raychaudhuri, G. Kobernik, K. Dorr, K.-H. Muller, L. Schultz, R. Pinto, Appl. Phys. Lett. 79 (2001) 2408.
[3] Y.G. Zhao, R.C. Srivastava, P. Fournier, V. Smolyaninova, M. Rajeswari, T. Wu, Z.Y. Li, R.L. Greene, T. Venkatesan, J. Magn. Magn. Mater. 220 (2000) 161.
[4] V.L. Joseph Joly, P.A. Joy, S.K. Date, J. Magn. Magn. Mater. 247 (2002) 316.
[5] J.-Y. Lin, W.J. Chang, J.Y. Juang, T.M. Wen, K.H. Wu, Y.S. Gou, J.M. Lee, J.M. Chen, J. Magn. Magn. Mater. 282 (2004) 237.
[6] G.T. Tan, S.Y. Dai, P. Duan, H.B. Lu, Y.L. Zhou, Z.H. Chen, Phys. Rev. B 68 (2003) 014426.
[7] P. Duan, G. Tan, S. Dai, Y. Zhou, Z. Chen, J. Phys.: Condens. Matter 15 (2003) 4469.
[8] P. Duan, S.Y. Dai, G.T. Tan, H.B. Lu, Y.L. Zhou, B.L. Cheng, Z.H. Chen, J. Appl. Phys. 95 (2004) 5666.
[9] P. Duan, Z. Chen, S. Dai, Y. Zhou, H. Lu, K. Jin, B. Cheng, Appl. Phys. Lett. 84 (2004) 4741.
[10] O. Mora′n, R. Hott, K. Grube, D. Fuchs, R. Schneider, E. Baca, W. Saldarriaga, P. Prieto, J. Appl. Phys. 95 (2004) 6239.
[11] M.E. Fischer, M.N. Bader, Phys. Rev. Lett. 28 (1972) 1516.
[12] S. Jin, T.H. Tiefel, M. McCormack, R.A. Fastnacht, R. Ramesh, L.H. Chen, Science 264 (1994) 413.
[13] J. Zhang, H. Tanaka, T. Kanki, J.-H. Choi, T. Kawai, Phys. Rev. B 64 (2001) 184404.
[14] C. Mitra, P. Raychaudhuri, J. John, S.K. Dhar, A.K. Nigam, R. Pinto, J. Appl. Phys. 89 (2001) 524.
[15] X. Guo, S. Dai, Y. Zhou, G. Yang, Z. Chen, Appl. Phys. Lett. 75 (1999) 3378.
[16] A. Urushibara, Y. Moritomo, T. Arima, A. Asamitsu, G. Kido, Y. Tokura, Phys. Rev. B 51 (1995) 14103.
[17] I. Mannari, Progr. Theoret. Phys. 22 (1959) 335.
[18] S. Bhattacharya, S. Pal, A. Banerjee, H.D. Yang, B.K. Chaudhuri, J. Chem. Phys. 119 (2003) 3972.
[19] M. Jaime, M.B. Salamon, M. Rubinstein, R.E. Treece, J.S. Horowitz, D.B. Chrisey, Phys. Rev. B 54 (1996) 11914.
[20] H.Y. Hwang, S-W. Cheong,, N. P. Ong, B. Batlogg, Phys. Rev. Lett. 77 (1996) 2041.
[21] H. Guo, Z. Chen, L. Liu, S. Ding, Y. Zhou, H. Lu, K. Jin, B. Cheng, Appl. Phys. Lett. 85 (2004) 3172.
[22] S. Chatterjee, A.K. Nigam, Phys. Rev. B 66 (2002) 104403.
[23] A. Chainani, M. Mathew, D.D. Sarma, Phys. Rev. B 47 (1993) 15397.
[24] J. Yeh, I. Lindau, Data Nucl. Data Tables 32 (1985) 1.
[25] S. Lütkehoff, M. Neumann, Phys. Rev. B 52 (1995) 13808.
[26] A. Bianconi, A. Kotani, K. Okada, R. Giorgi, A. Gargano, A. Marcelli, T. Miyahara, Phys. Rev. B 38 (1988) 3433.